JOURNAL OF GUIDANCE, CONTROL, AND DYNAMICS
Vol. 32, No. 3, May–June 2009

Engineering Notes

ENGINEERING NOTES are short manuscripts describing new developments or important results of a preliminary nature. These Notes should not exceed 2500 words (where a figure or table counts as 200 words). Following informal review by the Editors, they may be published within a few months of the date of receipt. Style requirements are the same as for regular contributions (see inside back cover).

Pseudospectral Motion Planning for Autonomous Vehicles

Qi Gong*
University of California, Santa Cruz, Santa Cruz, California 95064
and
L. R. Lewis† and I. Michael Ross‡
Naval Postgraduate School, Monterey, California 93943

DOI: 10.2514/1.39697

I. Introduction

A COMMON task for autonomous vehicles is motion planning. Discipline-based design of motion planning algorithms have led to the development and evolution of different techniques to solve specific problems. For instance, the artificial–potential–function technique [1] is a popular method for the motion planning of unmanned ground vehicles (UGV) and robotic manipulators [1–3]. Although this technique has been used for over 30 years, it suffers from the possibility of the vehicle not achieving its goal and difficulties in accommodating various environmental constraints [4]. To overcome such issues, recent developments in motion planning algorithms place heavy emphasis on so-called sampling-based planning techniques such as probabilistic road maps, rapidly exploring random trees, and expansive space trees to name a few [5–9]. These methods use probabilistic means of connecting the initial configuration to the final configuration thereby enabling an improved capacity to achieve the goal and a capability to generate initial feasible paths. In all these techniques, the initial feasible paths do not automatically incorporate vehicle dynamics; hence, path-following control techniques are needed to satisfy the physics of the motion [9]. This is one reason why nonholonomic constraints play such a crucial role in constrained control techniques that are designed to serve path-following systems.

There is no doubt that optimal control theory is the most natural framework for solving motion planning problems; however, solving optimal control problems has historically been considered difficult due to the twin curses of dimensionality and complexity. These difficulties are exacerbated in the presence of state constraints; hence, an obstacle-cluttered environment becomes a substantially more difficult problem under the framework of optimal control theory [10,11]. Nonetheless, it is possible to solve simplified motion planning problems wherein the cost function is quadratic or the environment is obstacle free. Because the motion planning techniques developed in robotics applications are unsuitable for flight vehicles, such as launch and reentry, for example, aerospace problems have motivated the development of efficient optimal control algorithms. In aerospace applications, satisfaction of the dynamical constraints is exceedingly important; hence, trajectory and control become fundamentally intertwined. On the other hand, aerospace problems do not have the vast number of path constraints that are common in an obstacle-cluttered environment.

In recent years, paradigm-changing advancements have taken place in computational optimal control that challenge conventional wisdom. For instance, onboard the International Space Station, Bedrossian et al. [12] discovered and implemented a revolutionary momentum-dumping approach that they call a zero-propellant maneuver. This discovery was made possible by an application of pseudospectral methods to solve a real-life challenging optimal control problem [13]. Other applications of such advancements are discussed in [14,15] and include the ground test of a revolutionary attitude control concept for the NPSAT1 spacecraft. Motivated by these advancements, we apply pseudospectral methods to develop motion planning algorithms for autonomous vehicles characterized by nonlinear dynamical constraints, an obstacle-cluttered environment, and a need to generate solutions in real time.

We consider the problem of generating optimal trajectories for generic autonomous vehicles. Shapes of arbitrary number, size, and configuration are modeled in the form of path constraints in the resulting optimal control problem. The method is tested under various obstacle environments on different platforms such as sea surface vehicles, ground vehicles, and aerial vehicles. The optimality of the computed trajectories is verified by way of the necessary conditions. We show that it is possible to do motion planning for different problems under the unified framework of optimal control and pseudospectral methods [16–19].

II. Vehicle Types

A particularly attractive advantage of the proposed pseudospectral motion planning technique is its applicability to different platforms. To this end, consider three types of vehicles: unmanned ground vehicles, sea surface vehicles, and unmanned aerial vehicles.

A. Underactuated Ship

Let (x, y, ϕ) be the position and orientation of a ship in the Earth fixed frame, and let (v_1, v_2, r) be the velocities in surge, sway, and yaw directions. Consider the motion in only the horizontal plane. The dynamics of a ship can be described as [20]

$$\begin{aligned} &\dot{x} = v_1\cos\phi - v_2\sin\phi \qquad \dot{y} = v_1\sin\phi + v_2\cos\phi \qquad \dot{\phi} = r \\ &\dot{v}_1 = \frac{m_{22}}{m_{11}}v_2 r - \frac{d_{11}}{m_{11}}v_1 + \frac{1}{m_{11}}u_1 \qquad \dot{v}_2 = -\frac{m_{11}}{m_{22}}v_1 r - \frac{d_{22}}{m_{22}}v_2 \\ &\dot{r} = \frac{m_{11}-m_{22}}{m_{33}}v_1 v_2 - \frac{d_{33}}{m_{33}}r + \frac{1}{m_{33}}u_2 \end{aligned} \tag{1}$$

where m_{ii} are the ship's inertia terms with added mass effects, d_{ii} are the hydrodynamic damping coefficients, and (u_1, u_2) are the control forces in the surge and yaw directions subject to the constraints,

Received 10 July 2008; revision received 2 November 2008; accepted for publication 6 November 2008.

*Assistant Professor, Department of Applied Mathematics and Statistics; qigong@soe.ucsc.edu.
†Lieutenant, United States Navy, Department of Mechanical and Astronautical Engineering.
‡Professor, Department of Mechanical and Astronautical Engineering; imross@nps.edu. Associate Fellow AIAA.

$$u_{i,\min} \le u_i \le u_{i,\max}, \qquad i = 1, 2$$

The system is underactuated because there is no sway control force. Further discussions on such an underactuated ship model can be found in [20] and the references therein.

B. Nonholonomic Unmanned Ground Vehicle

Consider a four-wheeled car with rear-wheel drive and front-wheel steering; see Fig. 1. The nonholonomic nature of this system makes the motion planning problem difficult [5]. The x–y location of the car represents the center point of the rear axle. The car's orientation angle θ is measured with respect to the horizontal axis, the steering angle ϕ is measured with respect to the car's heading, or velocity vector, and L is the distance between the front and rear axles. The dynamical model for this system is given by [5]

$$\dot{x} = v\cos(\theta) \qquad \dot{y} = v\sin(\theta) \qquad \dot{\theta} = \frac{v}{L}\tan(\phi) \tag{2}$$

where the speed v and the steering angle ϕ are the control variables subject to constraints

$$v_{\min} \le v \le v_{\max} \qquad \phi_{\min} \le \phi \le \phi_{\max}$$

Note that, unlike the Reeds-Shepp car or the Dubins car, the velocity is allowed to change continuously similar to the capability of a real automobile.

C. Unmanned Aerial Vehicle

For an unmanned aerial vehicle (UAV) model (see Fig. 2), the state variables represent the 3 spatial degrees of freedom. The three control variables are the vehicle velocity v, the flight path angle γ, and the heading angle ξ. The flight path angle is measured from the local horizontal to the velocity vector; and the heading angle is measured from a reference heading (e.g., due north) to the velocity vector. A model for this dynamical system is given by

$$\dot{x} = v\cos(\gamma)\cos(\xi) \qquad \dot{y} = v\cos(\gamma)\sin(\xi) \qquad \dot{z} = v\sin(\gamma) \tag{3}$$

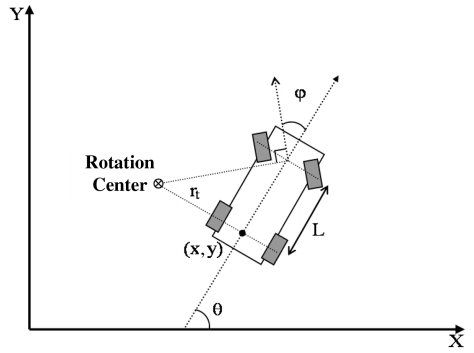

Fig. 1 A four-wheeled car with front-wheel steering.

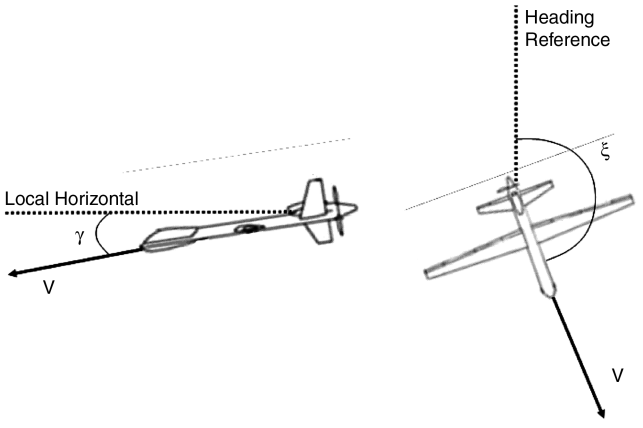

Fig. 2 Definition of UAV variables (modified from [36]).

III. Formulation of Optimal Path Planning Problem

One of the many advantages to using optimal control methods is the relative ease with which a multitude of problems can be formulated. Any kinematic, dynamic, or path constraint or optimality criterion that is appropriately expressed in a mathematical manner can be rapidly incorporated into the problem formulation. Thus, the key problem is to express the environmental characteristics appropriately so that the resulting optimal control problem can be solved efficiently.

A. Obstacle Representation

To mathematically represent the obstacles around which the vehicle must maneuver, path constraints are used in the optimal control formulation of motion planning problems. For simplicity and computational efficiency, it is desirable to represent the path constraints as differentiable algebraic functions. With this framework in mind, the p-norm,

$$\|(x, y)\|_p \triangleq (|x|^p + |y|^p)^{\frac{1}{p}}, \qquad p = 1, 2, \ldots$$

is used to create generic shapes such as diamonds, circles, ellipses, squares, and rectangles. Figure 3 illustrates how the p-norm can be manipulated to create a diamond, a circle, and a square obstacle. Ellipses and rectangles are simply extensions of the circle and square, respectively, where the distance along the x and y axes is dissimilar. This technique can be extended to cover more general polygonal obstacle shapes and 3-D obstacles [21].

Within the context of optimal control theory, the obstacles in a 2-D plane can be represented by the following path constraints:

$$h(x, y) = \left\| \left(\frac{x - x_c}{a}, \frac{y - y_c}{b} \right) \right\|_p - c \ge 0$$

where (x_c, y_c) is the center of the obstacle and (a, b, c) are constant parameters. If a large value of p is chosen, the value of h becomes too large; hence, for computational efficiency, we scale the path constraint by the logarithmic function as

$$\log\left(\left(\frac{x - x_c}{a} \right)^p + \left(\frac{y - y_c}{b} \right)^p \right) \ge p \log c$$

B. Problem Formulation

In a typical motion planning problem, the cost function is the distance traversed. Because the shortest path is not necessarily the minimum-time path, it is desirable to formulate an optimal path planning problem with an appropriate cost function that depends on the application at hand; hence, we formulate an optimal obstacle-avoidance problem for a generic vehicle as a constrained optimal control problem with a generic Bolza cost function.

Optimal Path Planning: Determine the state-control function pair, $t \mapsto (\boldsymbol{x}, \boldsymbol{u}) \in \mathbb{R}^{N_x} \times \mathbb{R}^{N_u}$, and final time, t_f, that minimize the cost functional

$$J[\boldsymbol{x}(\cdot), \boldsymbol{u}(\cdot), t_f] = E(\boldsymbol{x}(t_0), \boldsymbol{x}(t_f), t_f) + \int_{t_0}^{t_f} F(\boldsymbol{x}(t), \boldsymbol{u}(t))\, \mathrm{d}t$$

subject to vehicle dynamics

$$\dot{\boldsymbol{x}} = \boldsymbol{f}(\boldsymbol{x}, \boldsymbol{u})$$

boundary conditions,

$$\boldsymbol{e}_0(\boldsymbol{x}(t_0)) = \boldsymbol{0}, \qquad \boldsymbol{e}_f(\boldsymbol{x}(t_f), t_f) = \boldsymbol{0}$$

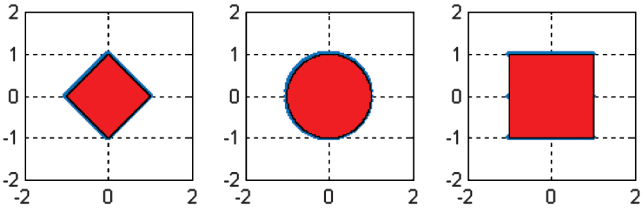

Fig. 3 Unit p-norms for $p = 1$, 2, 100, respectively.

control constraints,

$$\boldsymbol{u}_{\min} \le \boldsymbol{u} \le \boldsymbol{u}_{\max}$$

and path constraints,

$$\mathbf{0} \le \mathbf{h}(\boldsymbol{x})$$

where h_i, the ith component of $\mathbf{h}$, represents the ith obstacle.

This optimal control formulation of a motion planning problem covers a large variety of applications. First, the consideration of general nonlinear dynamics allows different vehicles. Because there is no simplification on the nonlinear dynamics, the resulting trajectory is automatically guaranteed to be feasible with respect to the vehicle dynamics. In some applications, due to the limitations on the actuators, a smooth controller may be desirable. Such requirements can easily be incorporated by augmenting a dummy control, v, and forcing $\dot{u} = v$. Second, the choice of cost function can be very general and not necessarily limited to be a quadratic. Thus, for example, it can be chosen freely to represent the true requirements such as a minimum transfer time. Third, the obstacles as well as other physical constraints such as limitations on the velocity and steering angles can be easily represented in an optimal control formulation by way of generic nonlinear path constraints. Because of the flexibility provided by constrained nonlinear optimal control, this approach can deal with a large variety of engineering motion planning problems in a unified manner. Of course, a successful application of this approach relies heavily on an efficient computational algorithm.

IV. Pseudospectral Methods

In this section we summarize the basic principles of pseudospectral (PS) methods. Over the last decade, PS methods have moved rapidly from theory [16,22] to practice [14,23–27] to flight and industrial applications [12–15]. PS methods are particularly attractive for autonomous trajectory planning as its efficiency places real-time computation within easy reach of onboard computer systems [28]. Recent advances on PS methods can be found in [16,17,19].

We take the Legendre PS method as an illustrative method while noting that the results are applicable to other PS methods as well [29]. In the Legendre PS method, we approximate $\boldsymbol{x}(t)$ by Nth order Lagrange polynomials $\boldsymbol{x}^N(t)$ based on interpolation at the shifted Legendre–Gauss–Lobatto (LGL) quadrature nodes, that is,

$$\boldsymbol{x}(t) \approx \boldsymbol{x}^N(t) = \sum_{k=0}^{N} \boldsymbol{x}^N(t_k)\phi_k(t)$$

where $t_k = (t_f - t_o/2)(\tau_k + 1)$ are the shifted LGL nodes with τ_k defined as $\tau_0 = -1$, $\tau_N = 1$, τ_k, for $k = 1, 2, \ldots, N-1$, are the roots of the derivative of the Nth order Legendre polynomial, and $\phi_k(t)$ are the Lagrange interpolating polynomials. The derivative of the ith state $x_i(t)$ at the LGL node t_k is approximated by

$$\dot{x}_i(t_k) \approx \dot{x}_i^N(t_k) = \sum_{j=0}^{N} D_{kj} x_i^N(t_j), \qquad i = 1, 2, \ldots, N_x$$

where D is the $(N+1) \times (N+1)$ differentiation matrix defined as

$$D_{ik} = \frac{2}{t_f - t_0} \begin{cases} \frac{L_N(\tau_i)}{L_N(\tau_k)} \frac{1}{\tau_i - \tau_k}, & \text{if } i \ne k \\ -\frac{N(N+1)}{4}, & \text{if } i = k = 0 \\ \frac{N(N+1)}{4}, & \text{if } i = k = N \\ 0, & \text{otherwise} \end{cases}$$

Let $\bar{x}_k = x^N(t_k)$, $k = 0, 1, \ldots, N$. The "bar" notation is used to denote discretized variables. Note that the subscript in $\bar{\boldsymbol{x}}_k$ denotes an evaluation of the approximate state, $\boldsymbol{x}^N(t) \in \mathbb{R}^{N_x}$, at the node t_k whereas $x_k(t)$ denotes the kth component of the exact state. The differential equation is approximated by the following nonlinear algebraic inequalities:

$$\left\| \sum_{i=0}^{N} \bar{x}_i D_{ki} - f(\bar{\boldsymbol{x}}_k, \bar{\boldsymbol{u}}_k) \right\|_\infty \le \delta \tag{4}$$

where $\delta > 0$ is a small number representing the feasibility tolerance; and $\|\cdot\|_\infty$ denotes the maximum component of a vector. The endpoint conditions and constraints are approximated in a similar fashion

$$\|\boldsymbol{e}_0(\bar{x}_0)\|_\infty \le \delta \quad \|\boldsymbol{e}_f(\bar{x}_N, t_N)\|_\infty \le \delta \quad \mathbf{h}(\bar{\boldsymbol{x}}_k) \ge \delta \cdot \mathbf{1}, \quad k = 0, \ldots, N \tag{5}$$

where $\mathbf{1}$ denotes $[1, \ldots, 1]^T$. Finally, the cost functional $J[\boldsymbol{x}(\cdot), \boldsymbol{u}(\cdot), t_f]$ is approximated by the Gauss–Lobatto integration rule,

$$J[\boldsymbol{x}(\cdot), \boldsymbol{u}(\cdot), t_f] \approx \bar{J}^N = \frac{t_N - t_0}{2} \sum_{k=0}^{N} F(\bar{\boldsymbol{x}}_k, \bar{\boldsymbol{u}}_k) w_k + E(\bar{\boldsymbol{x}}_0, \bar{\boldsymbol{x}}_N, t_N) \tag{6}$$

where w_k are the LGL weights given by

$$w_k = \frac{2}{N(N+1)} \frac{1}{[L_N(\tau_k)]^2}$$

$k = 0, 1, \ldots, N$. Because practical solutions are bounded, the following constraints are added $\{\bar{\boldsymbol{x}}_k \in \mathbb{X}, \bar{\boldsymbol{u}}_k \in \mathbb{U}, t_N \in \mathbb{T}\}$, $k = 0, 1, \ldots, N$, where $\mathbb{X}$, $\mathbb{U}$, and $\mathbb{T}$ are compact sets representing the search region. Hence, the optimal motion planning is approximated by the following:

Problem B^N: Find $\bar{\boldsymbol{x}}_k \in \mathbb{X}$, $\bar{\boldsymbol{u}}_k \in \mathbb{U}$, $k = 0, 1, \ldots, N$, and $t_N \in \mathbb{T}$ that minimize the cost function (6), subject to constraints (4) and (5).

Problem B^N is solved by a spectral algorithm [19]. A version of this algorithm is implemented in the software package, DIDO [30]. All the results reported in this Note were computed using this implementation. Theoretical analysis on PS methods pertaining to feasibility and consistency of the approximation can be found in [16,18,31].

V. Results

We first present results for a basic motion planning problem for a sea surface vehicle. The optimality of the solution is analyzed by way of Pontryagin's principle. Note, however, that Pontryagin's principle is not explicitly used in PS methods; rather, all the dual variables are obtained by way of the covector mapping theorem [18,22,31].

A. Basic Obstacle-Avoidance Problem for Underactuated Ship

Consider the ship model described in Eq. (1). The parameters used in the simulations are taken from [32]. An optimal obstacle-avoidance problem is evaluated for the purposes of displaying the feasibility and optimality of the proposed solution approach. In x–y coordinates, the ship is intended to travel from an initial location, (100 m, 100 m), to the final location, (0, 0), while staying away from an elliptic obstacle modeled by

$$h(x, y) = (2x - 100)^2 + (y - 50)^2 - 40^2 \ge 0$$

The initial velocities are all zeros and the initial orientation is $5\pi/4$. The final velocities and orientation are

$$[\phi(t_f), v_1(t_f), v_2(t_f), r(t_f)] = (\pi, 0 \text{ m/s}, 0 \text{ m/s}, 0 \text{ rad/s})$$

The final time is free within $t_f \in [0, 300 \text{ s}]$. The control forces are subject to the constraints

$$-50 \text{ kN} \le u_1(t) \le 50 \text{ kN} \qquad -50 \text{ kN} \le u_2(t) \le 50 \text{ kN}$$

We formulate the obstacle-avoidance problem as a constrained optimal control problem with a quadratic energy-like cost function

$$J[x(\cdot), u(\cdot), t_f] = \int_0^{t_f} u_1^2(t) + (0.1u_2)^2(t)\, \mathrm{d}t$$

The candidate optimal control trajectory for 64 nodes is shown in Fig. 4. When the controls are interpolated and the initial state is propagated through the system dynamics, we arrive at a candidate state trajectory. This ship trajectory is shown in Fig. 5. Also shown in Fig. 5 is the ship trajectory for 64 nodes. Because the distance between the propagated trajectory and PS-generated trajectory is less than 0.034 m, the two trajectories are visually indistinguishable in Fig. 5.

To investigate the optimality of the computed solution, we apply Pontryagin's minimum principle. From the Hamiltonian minimization condition, it is quite straightforward to show that the candidate optimal controller must satisfy,

$$u_1^*(t) = s_1(t), \quad \text{if } -50 \text{ KN} < s_1(t) = -0.5\lambda_{v1}(t)/m_{11} < 50 \text{ KN}$$

$$u_2^*(t) = 50 \text{ KN}, \quad \text{if } s_2(t) = 0.02u_2^*(t) + \lambda_r(t)/m_{33} < 0$$

$$u_2^*(t) = -50 \text{ KN}, \quad \text{if } s_2(t) = 0.02u_2^*(t) + \lambda_r(t)/m_{33} > 0$$

Figure 6 displays the value of the switching functions $s_1(t)$ and $s_2(t)$, where the costates are computed using the covector mapping theorem [18,22]. Clearly, the candidate optimal control satisfies the Hamiltonian minimization condition.

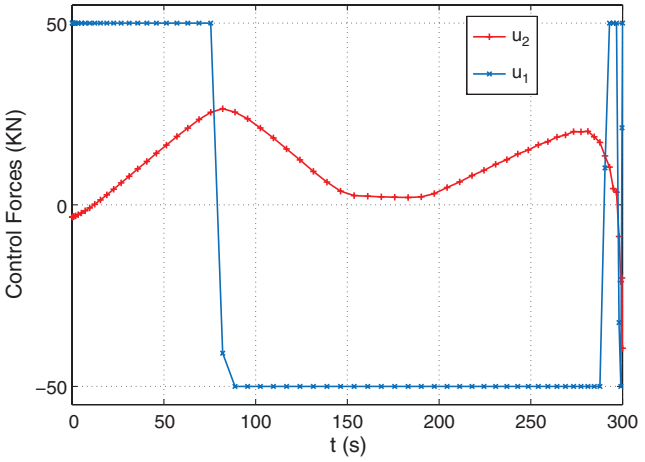

Fig. 4 Candidate optimal controls for obstacle avoidance.

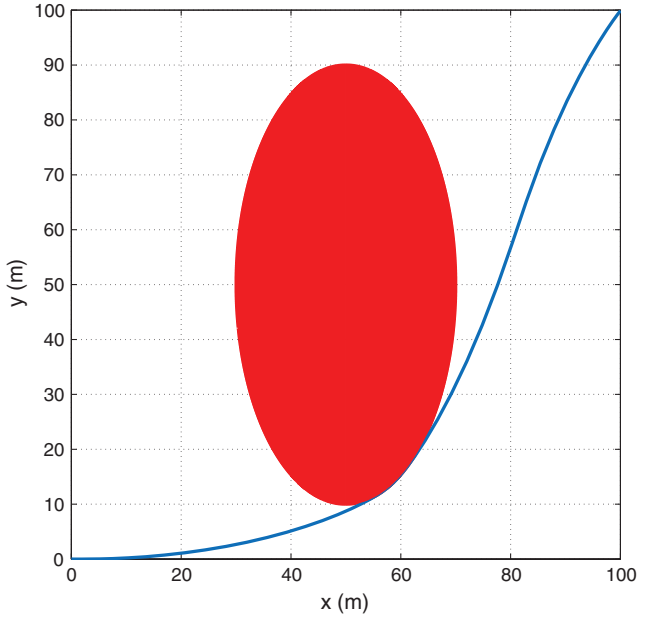

Fig. 5 Optimal ship trajectory for an elliptic obstacle.

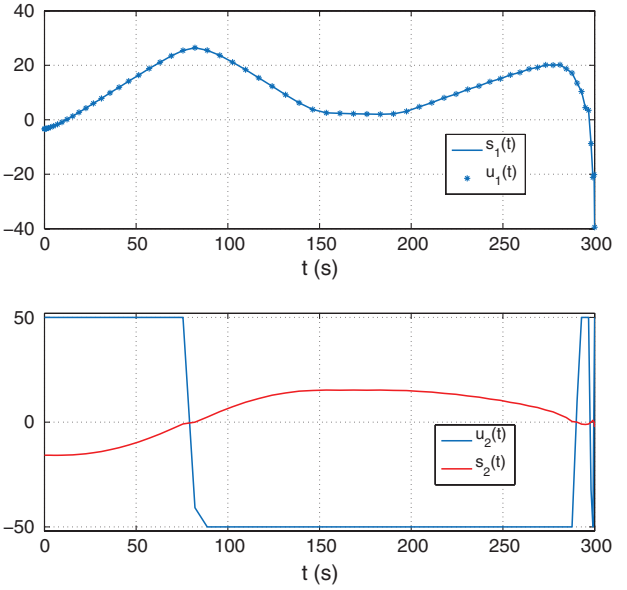

Fig. 6 Switching function and the candidate optimal control.

B. Unmanned Ground Vehicle Path Planning in Obstacle-Cluttered Environment

In this section, we demonstrate the proposed algorithm for the motion planning of an UGV navigating through an obstacle-cluttered environment. All examples are formulated as time-optimal control problems, that is, minimizing the transfer time that takes the vehicle from its initial position to the final position. The velocity is between $[-0.2 \text{ m/s}, 0.2 \text{ m/s}]$ and the steering angle ϕ is within $[-35 \text{ deg}, 35 \text{ deg}]$. The parameter L in system (2) is 0.1 m. The details of these examples can be found in [21,33]. The units, in all the figures shown in this section, are in meters.

Figure 7a shows a time-optimal trajectory generated against a multishape obstacle environment. These obstacles are mathematically modeled by the p-norm concept introduced in the previous section. The vehicle travels in straight lines except when it just touches an obstacle. Figure 7b demonstrates the applicability of optimal control techniques in an obstacle-cluttered environment where 32 circular obstacles are incorporated. For the purpose of brevity, we do not illustrate the optimality tests but refer to [21] for further results and analysis.

Now suppose that the UGV is defective in such a manner that it can turn only left, that is, the steering angle is always positive. In such a case, the only thing that needs to be changed in the proposed algorithm is the lower bound on the steering angle. Our solution is shown in Fig. 8. The time-optimal result requires two types of motion. The first type combines forward motion of the vehicle with a minimum steering angle; this results in a maximum turning radius. The second type of motion combines the backward motion of the vehicle with a maximum steering angle; this results in a minimum

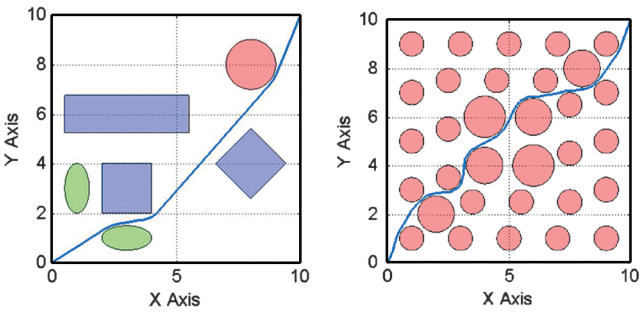

a) Multishape obstacle environment **b) Obstacle-cluttered environment**

Fig. 7 Time-optimal trajectory for a nonholonomic UGV in an obstacle-cluttered environment.

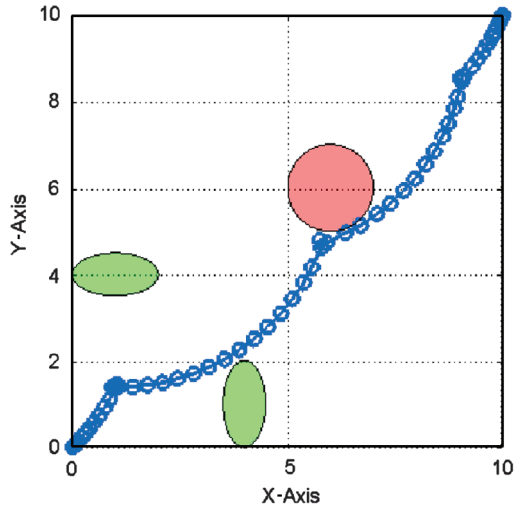

Fig. 8 Time-optimal UGV maneuver with wheel-control failure.

turning radius. In total, the UGV moves forward with a minimum turning radius and then backward with the maximum turning radius to align for the next forward motion. This type of motion is used in a repetitive fashion in Fig. 8 to successfully navigate around the obstacles.

Finally, we consider the interesting problem of parallel parking. After representing the obstacles as path constraints, the parallel parking problem becomes a routine optimal control problem provided the size of the vehicle is accounted for correctly; no further work is required. Our solution to the time-optimal problem is shown in Figs. 9 and 10. This solution is quite different to that of a human driver where the standard rule is to move the vehicle past the parking space and back it down. A closer inspection of the time-optimal maneuver (see Fig. 10) reveals that the number of turns required to do the time-optimal maneuver is more than the standard three-point turn used by typical human drivers. This result explains why most human drivers chose to back down into a parking spot rather than move up. Additional results on UGV motion planning using PS methods can be found in [34].

C. Optimal Path Planning for Unmanned Aerial Vehicle in Urban Environment

Consider the problem of navigating a small UAV through an urban environment. This problem is more complex than that of a larger UAV flying at a high altitude and away from obstacles.

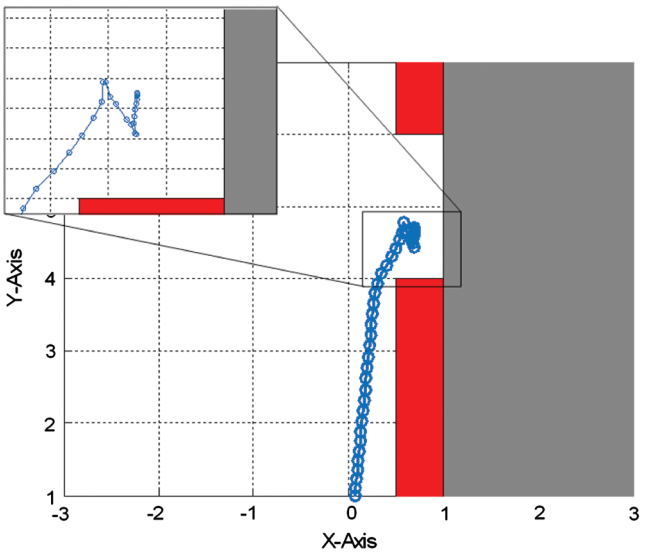

Fig. 10 Top view of a forward parallel parking maneuver.

We consider six 3-D structures representing a city environment as shown in Fig. 11. The buildings are model using a p-norm with $p = 100$. The initial and final conditions are

$$[x(t_0), y(t_0), z(t_0)] = (0, 0, 25\ \text{m})$$

$$[x(t_f), y(t_f), z(t_f)] = (100\ \text{m}, 100\ \text{m}, 10\ \text{m})$$

The velocity is bounded by

$$3\ \text{m/s} \leq v(t) \leq 10\ \text{m/s}$$

The minimum-time solution for this problem is shown in Fig. 11. The units in these plots are scaled with 1 unit = 10 m.

Because of its 3-D nature, the time-optimal solution to the problem is shown from multiple viewing perspectives in Fig. 11. From the top view (x–y plane), it appears that the UAV collides with one of the buildings; however, the view in x–z plane clearly shows that the trajectory goes above the building, thus avoiding all the obstacles. A detailed feasibility and optimality analysis can be found in [21]. Additional results for other types of flying platforms can be found in [35].

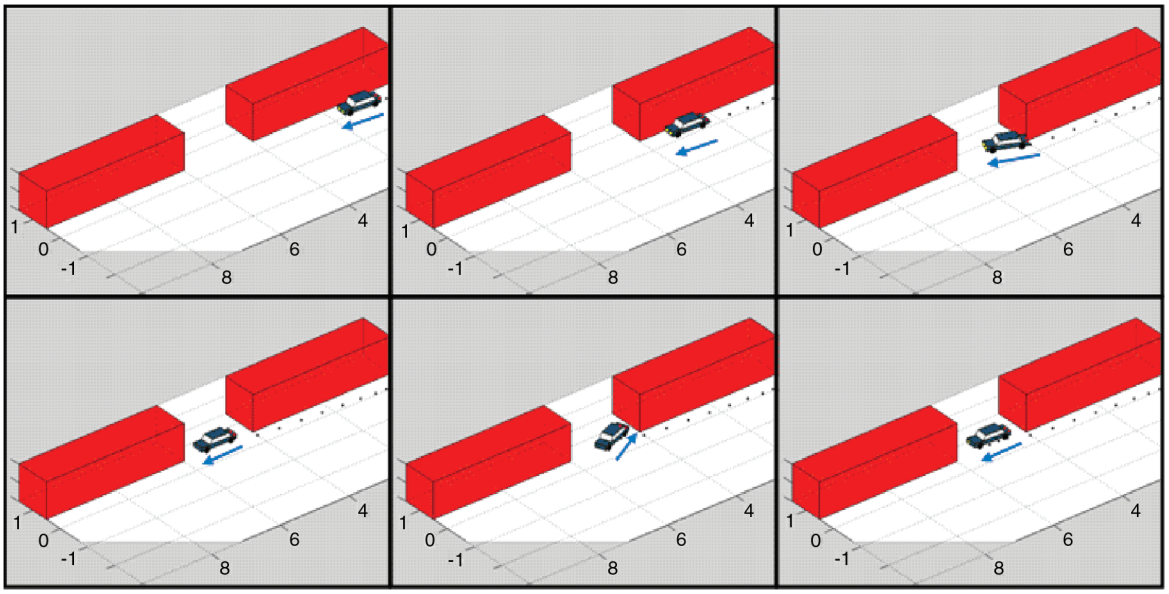

Fig. 9 Scenes from a forward parallel parking maneuver.

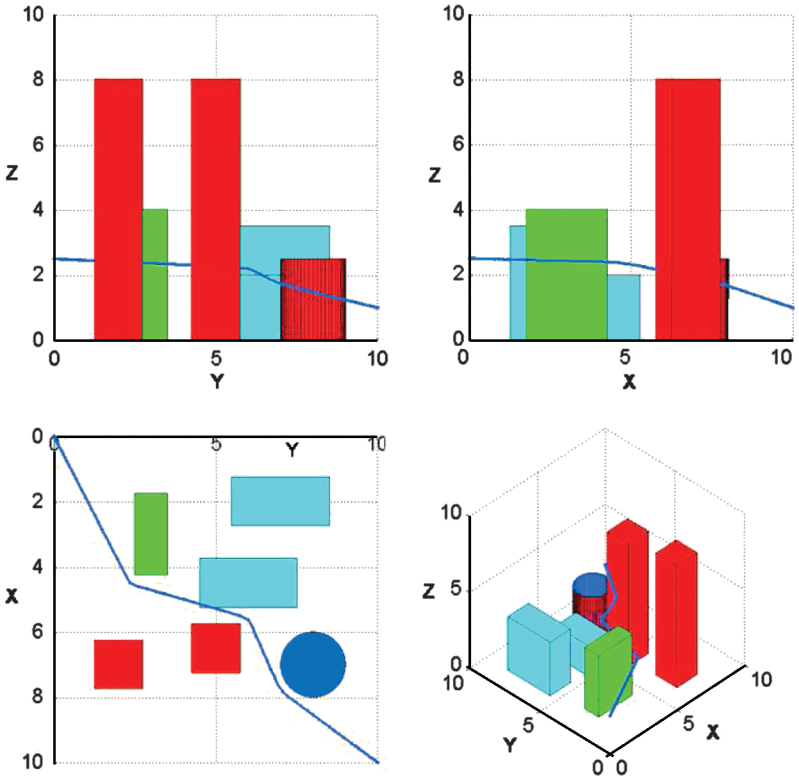

Fig. 11 Time-optimal UAV trajectory in an urban environment.

D. Computational Time

All problems in this Note were programmed in MATLAB by way of DIDO [30] running on an Intel based MacBook Pro laptop with 2 GB of RAM. The computational time for the ship motion planning problem was about 30 s. For UGV and UAV problems, the computational time was about 15 s. It is possible to improve the computational time in a variety of different ways [28]; for instance, if the computational overhead associated with the Windows operating system and the MATLAB environment is removed, substantial speed improvements are possible. As shown in [28], it is even possible to obtain solutions as fast as 30 Hz. Thus, the proposed motion planning technique can indeed be used in a real-time fashion to handle a dynamic environment as well as compensate for uncertainties. Preliminary results along this direction are reported in [21,34].

VI. Conclusions

Through various examples, we demonstrated a unified optimal motion planning algorithm for heterogeneous vehicles navigating through an obstacle-cluttered environment. These optimal solutions do not mimic human rules; thus, motion planning algorithms that purport to mimic human rules do not provide the best solutions and may also create unintended problems such as conflicts between rules. In an optimal control approach, solutions can be obtained quite seamlessly and even more intelligently than with a human driver as demonstrated in the case of an unmanned car.

References

[1] Khatib, O., "Real-Time Obstacle Avoidance for Manipulators and Mobile Robots," *The International Journal for Robotics Research*, Vol. 5, No. 1, 1986, pp. 90–98.

[2] Barraquand, J., Langlois, B., and Latombe, J., "Numerical Potential Field Techniques for Robot Path Planning," *IEEE Transactions on Systems, Man, and Cybernetics*, Vol. 22, No. 2, March/April 1992, pp. 224–241

[3] Shimoda, S., Kuroda, Y., and Iagnemma, K., "Potential Field Navigation of High Speed Unmanned Ground Vehicles on Uneven Terrain," *Proceedings International Conference on Robotics and Automation*, IEEE Publications, Piscataway, NJ, 2005, pp. 2828–2833.

[4] Zefran, M., "Continuous Methods for Motion Planning," Ph.D. Dissertation, University of Pennsylvania, Philadelphia, PA, Dec. 1996, pp. 1–14.

[5] Choset, H., Lynch, K. M., Hutchinson, S., Kantor, G., Burgard, W., Kavraki, L. E., and Thrum, S., *Principles of Robot Motion; Theory, Algorithms, and Implementation*, MIT Press, Cambridge, MA, 2005.

[6] LaValle, S. M., *Planning Algorithms*, Cambridge University Press, Cambridge, England, 2006.

[7] LaValle, S. M., and Kuffner, J. J., "Randomized Kinodynamic Planning," *International Journal of Robotics Research*, Vol. 20, No. 5, May 2001, pp. 378–400.

[8] Kavraki, L. E., Latombe, J. C., Svestka, P., and Overmars, M. H., "Probabilistic Roadmaps for Path Planning in High-Dimensional Configuration Spaces," *IEEE Tranactions on Robotics and Automation*, Vol. 12, No. 4, June 1996, pp. 566–580.

[9] LaValle, S. M., *From Dynamic Programming to RRTs: Algorithmic Design of Feasible Trajectories, Control Problems in Robotics*, Springer–Verlag, Berlin, 2002, pp. 19–37.

[10] Duleba, I., and Sasiadek, J., "Nonholonomic Motion Planning Based on Newton Algorithm with Energy Optimization," *IEEE Transactions on Control Systems Technology*, Vol. 11, No. 3, 2003, pp. 355–363. doi:10.1109/TCST.2003.810394

[11] Sasiadek, J., and Duleba, I., "3D Local Trajectory Planner for UAV," *Journal of Intelligent and Robotic Systems: Theory and Applications*, Vol. 29, Oct. 2000, pp. 191–210. doi:10.1023/A:1008108910932

[12] Bedrossian, N., Bhatt, S., Lammers, M., Nguyen, L., and Zhang, Y., "First Ever Flight Demonstration of Zero Propellant Maneuver Attitude Control Concept," AIAA Paper 2007-6734, 2007.

[13] Kang, W., and Bedrossian, N., "Pseudospectral Optimal Control Theory Makes Debut Flight," SIAM News, Vol. 40, No. 7, Sept. 2007.

[14] Ross, I. M., Sekhavat, P., Fleming, A., and Gong, Q., "Optimal Feedback Control: Foundations, Examples and Experimental Results for a New Approach," *Journal of Guidance, Control, and Dynamics*, Vol. 31, No. 2, 2008, pp. 307–321. doi:10.2514/1.29532

[15] Gong, Q., Kang, W., Bedrossian, N., Fahroo, F., Sekhavat, P., and Bollino, K., "Pseudospectral Optimal Control for Military and Industrial Applications," *Proceedings of the 46th IEEE Conference on Decision and Control*, IEEE Publications, Piscataway, NJ, Dec. 2007, pp. 4128–4142.

[16] Gong, Q., Kang, W., and Ross, I. M., "A Pseudospectral Method for the Optimal Control of Constrained Feedback Linearizable Systems," *IEEE Transactions on Automatic Control*, Vol. 51, No. 7, July 2006,

pp. 1115–1129.
doi:10.1109/TAC.2006.878570
[17] Ross, I. M., and Fahroo, F., "Advances in Pseusospectral Methods," AIAA Paper 2008-7309, Aug. 2008.
[18] Gong, Q., Ross, I. M., Kang, W., and Fahroo, F., "Connections Between the Covector Mapping Theorem and Convergence of Pseudospectral Methods for Optimal Control," *Computational Optimization and Applications*, 2008 (to be published).
[19] Gong, Q., Fahroo, F., and Ross, I. M., "A Spectral Algorithm for Pseudospectral Methods in Optimal Control," *Journal of Guidance, Control, and Dynamics*, Vol. 31, No. 3, 2008, pp. 460–471.
doi:10.2514/1.32908
[20] Lefeber, E., Pettersen, K. Y., and Nijmeijer, H., "Tracking Control of an Underactuated Ship," *IEEE Transaction on Control Systems Technology*, Vol. 11, No. 1, Jan. 2003, pp. 52–61.
doi:10.1109/TCST.2002.806465
[21] Lewis, L. R., "Rapid Motion Planning and Autonomous Obstacle Avoidance for Unmanned Vehicles," M.S. Thesis, Naval Postgraduate School, Monterey, CA, Dec. 2006.
[22] Fahroo, F., and Ross, I. M., "Costate Estimation by a Legendre Pseudospectral Method," *Journal of Guidance, Control, and Dynamics*, Vol. 24, No. 2, 2001, pp. 270–277.
doi:10.2514/2.4709
[23] Hawkins, A. M., Fill, T. R., Proulx, R. J., and Feron, E. M., "Constrained Trajectory Optimization for Lunar Landing," AAS, 06-153, Jan. 2006.
[24] Lu, P., Sun, H., and Tsai, B., "Closed-Loop Endoatmospheric Ascent Guidance," *Journal of Guidance, Control, and Dynamics*, Vol. 26, No. 2, 2003, pp. 283–294.
doi:10.2514/2.5045
[25] Williams, P., "Application of Pseudospectral Methods for Receding Horizon Control," *Journal of Guidance, Control, and Dynamics*, Vol. 27, No. 2, 2004, pp. 310–314.
doi:10.2514/1.5118
[26] Infeld, S. I., and Murray, W., "Optimization of Stationkeeping for a Libration Point Mission," AAS, Paper 04-150, Feb. 2004.
[27] Stanton, S., Proulx, R., and D'Souza, C., "Optimal Orbit Transfer Using a Legendre Pseudospectral Method," AAS Paper 03-574, 2003.
[28] Ross, I. M., and Fahroo, F., "Issues in the Real-Time Computation of Optimal Control," *Mathematical and Computer Modelling*, Vol. 43, No. 9–10, 2006, pp. 1172–1188.
doi:10.1016/j.mcm.2005.05.021
[29] Fahroo, F., and Ross, I. M., "Direct Trajectory Optimization by a Chebyshev Pseudospectral Method," *Journal of Guidance, Control, and Dynamics*, Vol. 25, No. 1, 2002, pp. 160–166.
doi:10.2514/2.4862
[30] Ross, I. M., *User's Manual for DIDO: A MATLAB Application Package for Solving Optimal Control Problems*, Elissar, Monterey, CA, 2007.
[31] Gong, Q., Ross, I. M., Kang, W., and Fahroo, F., "On the Pseudospectral Covector Mapping Theorem for Nonlinear Optimal Control," *IEEE Conference on Decision and Control*, IEEE Publications, Piscataway, NJ, Dec. 2006, pp. 2679–2686.
[32] Do, K. D., Jiang, Z. P., and Pan, J., "Underactuated Ship Global Tracking Under Relaxed Conditions," *IEEE Transactions on Automatic Control*, Vol. 47, No. 9, 2002, pp. 1529–1536.
doi:10.1109/TAC.2002.802755
[33] Lewis, L. R., and Ross, I. M., "A Pseudospectral Method for Real-Time Motion Planning and Obstacle Avoidance," *AVT–SCI Joint Symposium on Platform Innovations and System Integration for Unmanned Air, Land and Sea Vehicles*, NATO, 14–17 May 2007.
[34] Hurni, M. A., Sekhavat, P., and Ross, I. M., "Autonomous Trajectory Planning Using Real-Time Information Updates," AIAA Paper 2008-6305, Aug. 2008.
[35] Bollino, K. P., Lewis, L. R., Sekhavat, P., and Ross, I. M., "Pseudospectral Optimal Control: A Clear Road for Autonomous Intelligent Path Planning," *AIAA Infotech@Aerospace 2007 Conference and Exhibit*, AIAA, Reston, VA, 7–10 May 2007.
[36] General Atomics Aeronautical Systems, "Aircraft Platforms: Altair," http://www.ga-asi.com/products/index.php, 26 Oct. 2006.